

The self-adjusting current-fed push-pull parallel resonant inverter as a high frequency AC bus driver

Mor Mordechai Peretz and Sam Ben-Yaakov*

*Power Electronics Laboratory, Department of Electrical and Computer Engineering,
Ben-Gurion University of the Negev, Beer-Sheva 84105, Israel*

** Corresponding author: sby@ee.bgu.ac.il*

Received 1 March 2005, accepted 17 August 2005

Abstract

A self-adjusting sinusoidal power source for high-frequency AC distributed power bus is presented and tested experimentally. The power inverter is based on a Current-Fed Push-Pull Parallel-Resonant Inverter (CFPPRI), which includes a variable inductor and a frequency tracking mechanism to insure soft switching. The power source can drive reactive, non-linear, switched, and non-constant loads with a sinusoidal signal at a desirable frequency. The response of the power driver to a 60% to 100% step in the load power was found to stabilize within three high frequency cycles.

1 Introduction

A distributed power supply system includes a bus that spreads the primary power to the subunits, and on-board switch-mode converters that generate the required local supply voltages. The distributed power supply approach has several advantages over the central power supply solution: it reduces voltage drops due to high ground currents, facilitates isolation and thereby reduces common mode interferences, increases reliability, and distributes the power loss. At present, practically all distributed power supply systems

apply a DC bus, but similar to the reason why the power line is AC, there are advantages of using a high frequency AC bus (HFAC). The main advantage of an HFAC is the possibility of applying high frequency transformer at the input of the on board converters and thereby simplifying the isolation circuitry.

Notwithstanding the fact that the use of a HFAC bus for distributing power eliminates some of the conversion units, it poses new design challenges [1]: (a) electromagnetic interference, (b) bus waveshape – performance and efficiency of the load converters may be dramatically reduced due to a supply signal that is rich in harmonic content, and (c) point-of-load (POL) – the ability of the power source to drive various types of loads, such as reactive, non-linear, and non-constant.

The Self-Adjusting Current-Fed Push-Pull Parallel Resonant Inverter (SA-CFPPRI) was shown earlier [2,3] to be able to drive reactive loads with a sinusoidal output signal at a predetermined frequency and remain constant (amplitude and waveform wise) even for a non-constant reactive load (inductive and capacitive). This solves the first two challenges of the HFAC bus. In this study we explore the dynamics of the SA-CFPPRI loaded by a switched load, as expected in a HFAC distributed power source.

2 The current-fed push-pull parallel resonant inverter (CFPPRI)

The basic CFPPRI topology [4] (Fig. 1) includes a push-pull stage that consists of two transistors (Q_1, Q_2) fed by a series inductor (L_{in}), and drives a parallel resonant network. The load is fed via a secondary winding that allows for amplitude adjustment by the turns ratio ($n_2/2n_1$). The resonant frequency (f_r) of the parallel resonant network will be:

$$f_r = \frac{1}{2\pi\sqrt{L_m C_\Sigma}} \quad (1)$$

where L_m is the secondary inductance and C_Σ is the total capacitance reflected to the secondary ($C_1(n_2/2n_1)^2 + C_2 + C_L$).

2.1 Steady state operation

Out of symmetry considerations, only one-half cycle of operation will be described. It is assumed first that the switching frequency (f_s) is equal to the resonant frequency (f_r).

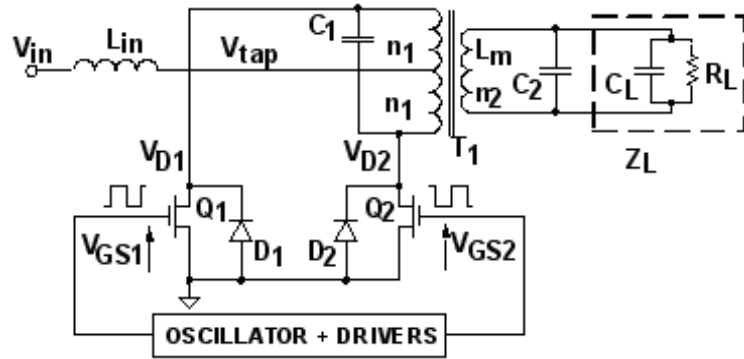


Figure 1: Basic configuration of the CFPPRI loaded by a capacitive load.

When the gate voltage of Q_1 (V_{GS1} , Fig. 1) goes high and the voltage of Q_2 (V_{GS2} , Fig. 1) goes low, the drain voltage of Q_1 (V_{D1} , Fig. 1) is forced to zero and the tank voltage (V_{D2} in this case) starts to rise in a sinusoidal shape. When this voltage reaches back to zero, switching occurs ($f_s = f_r$) and a new half cycle begins. In this case the transistors will operate under Zero Voltage Switching (ZVS) conditions (Fig. 2a). In the case that the switching frequency is lower than the resonant frequency (Fig. 2b), one of

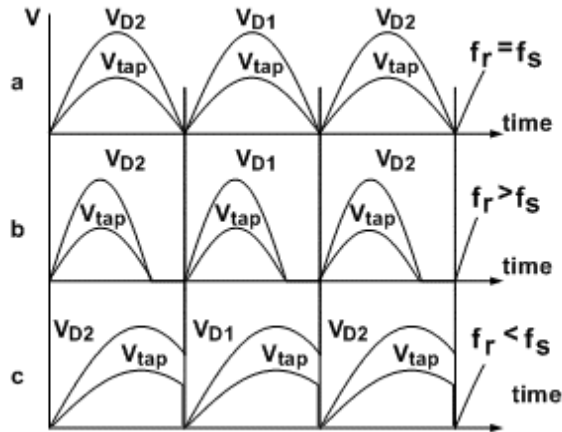


Figure 2: Drain voltages (V_D) and tap voltage (V_{tap}) when the gate-drive frequency matches the resonant frequency (a) and when it is lower (b) or higher (c) than the resonant frequency.

the antiparallel diodes will start conducting and the operation will include a boost period [4], which will cause distortion in the output voltage and increase conduction losses. If the switching frequency is higher than the resonant frequency (Fig. 2c), the operation will be under hard switching conditions. The functional circuit of the CFPPRI for one-half cycle is represented by the simplified equivalent circuit of Fig. 3a.

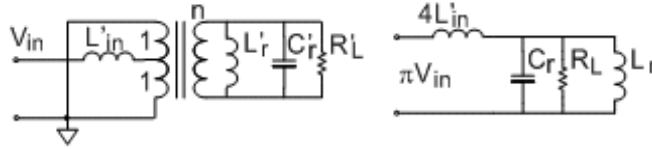


Figure 3: CFPPRI simplified circuit. (a) One-half cycle operation and (b) reflected to the primary.

2.2 Output voltage in steady state

Assuming that the resonant and the switching frequencies are equal and symmetry of one-half cycle, the output voltage will be sinusoidal and can be expressed as:

$$V_{Load}(t) = V_{Lpk} \cos(\omega_r t) \quad (2)$$

where V_{Lpk} is the load peak voltage and ω_r is the resonant frequency ($\omega_r = 2\pi f_r$).

After reflecting all components and signals to the primary winding (simplified reflected circuit is shown in Fig. 3b), the average center tap voltage (V_{tap} , Figs. 1 and 3) is given by:

$$V_{tapav} = \frac{1}{\pi} \int_{-\frac{T}{2}}^{\frac{T}{2}} \frac{V_{Lpk}}{n} \cos(\omega_r t) dt = \frac{2}{\pi} \frac{V_{Lpk}}{n} \quad (3)$$

where n is the turns ratio of the transformer T_1 of Fig. 1.

Since the average voltage across the input inductor (L_{in}) must be equal to zero at steady state, it can be stated that:

$$V_{tapav} = V_{in} \quad (4)$$

where V_{in} is the input voltage of the inverter.

Combining (3) and (4) and isolating V_{Lpk} , yields the peak output voltage in terms of the input voltage:

$$V_{Lpk} = n\pi \frac{V_{in}}{2}. \quad (5)$$

Eq. (5) implies that, in steady state, the load voltage is independent of the load value, which is a highly desirable feature for an HFAC distributed power bus driver.

2.3 Output voltage under transient conditions

Eq. (5) establishes the independence of the output voltage of the load in steady state. However, in the case of switched or non-constant loads, the system, which is of third order (LLC), will enter a transient period in which the output voltage will depend on the network characteristics. Out of symmetry considerations, one-half cycle operation will be analyzed, under the assumption that the next half cycle starts at the end of the previous cycle with no delay and is identical, except for an opposite direction of the resonant inductor (L_r) current.

The input inductor voltage is expressed by:

$$v_{in} - v_{L_r} = v_{L_{in}} \quad (6)$$

or,

$$v_{in} - L_r \frac{di_{L_r}}{dt} = L_{in} \frac{di_{L_{in}}}{dt} \quad (7)$$

where L_r is the resonant inductance and L_{in} is the input inductance reflected to the primary ($L_{in} = 4L_{in}'$).

Integrating (7) and isolating $i_{L_{in}}$, yields:

$$i_{L_{in}}(t) = \frac{v_{in}}{L_{in}}t - \frac{L_r}{L_{in}}(i_{L_r} - I_{L_r}(0)) + I_{in}(0) \quad (8)$$

where $I_{L_r}(0)$ and $I_{in}(0)$ are the initial conditions of the resonant inductor and the input inductor, respectively. Applying KCL, we derive:

$$i_{in} = i_{L_r} + i_{C_r} + i_{R_L} \quad (9)$$

where

$$v_{L_r} = v_{C_r} = v_{R_L} = L_r \frac{di_{L_r}}{dt},$$

$$i_{R_L} = \frac{V_L}{R_L} = \frac{L_r}{R_L} \frac{di_{L_r}}{dt}, \quad i_{C_r} = C_r \frac{dv_{C_r}}{dt} = L_r C_r \frac{d^2 i_{L_r}}{dt^2}.$$

Combining (8) and (9) and performing some manipulations, we obtain the complete differential equation of the CFPPRI for one-half cycle

$$\omega_n^2 \left(\frac{v_{in}}{L_{in}} t + \frac{L_r}{L_{in}} I_{L_r}(0) + I_{in}(0) \right) = i''_{L_r} + 2\alpha \cdot i'_{L_r} + (\omega_n^2 K^2) \cdot i_{L_r} \quad (10)$$

where $\omega_n = 1/\sqrt{L_r C_r}$ is the natural frequency, $\alpha = \omega_n/2Q$ is the damping coefficient, $Q = R_L/Z_r = R_L/\sqrt{L_r/C_r}$ is the quality factor, and $K = \sqrt{1 + L_r/L_{in}}$ is the error adjustment to the resonant frequency ($\omega_r = \omega_r K$) due to small input inductance value.

Solving (10) yields the expression for the resonant inductor current, $i_{L_r}(t)$:

$$i_{L_r}(t) = C e^{-\alpha t} \cos(\omega_r t - \phi_1) + D_1 t + D_0 \quad (11)$$

where

$$C = \sqrt{A^2 + B^2}; \quad \phi_1 = tg^{-1} \left(\frac{A}{B} \right); \quad B = i_{L_r}(0) - D_0; \quad A = \frac{B}{2Q} - \frac{D_1}{\omega_r};$$

$$D_1 = \frac{v_{in}}{L_{in}} \frac{1}{K^2}; \quad D_0 = \left(\frac{L_r}{L_{in}} I_{L_r}(0) + I_{in}(0) - \frac{v_{in}}{L_{in}} \frac{1}{K^2} \frac{1}{\omega_r Q} \right) \frac{1}{K^2}.$$

Taking the derivative of (11) and multiplying by L_r will yield the capacitor voltage, $v_{C_r}(t)$:

$$v_{L_r}(t) = v_{C_r}(t) = L_r \frac{di_{L_r}}{dt} \quad (12)$$

$$= L_r \left(-\alpha C e^{-\alpha t} \cos(\omega_r t - \phi_1) + \omega_r C e^{-\alpha t} \sin(\omega_r t - \phi_1) + D_1 \right)$$

or

$$v_{C_r}(t) = L_r \left(E e^{-\alpha t} \cos(\omega_r t - \phi_2) + D_1 \right)$$

where

$$E = -\sqrt{(\alpha C)^2 + (\omega_r C)^2} \quad ; \quad \phi_2 = \phi_1 - tg^{-1} \left(\frac{\omega_r}{\alpha} \right).$$

Normalizing (11) by considering V_{in} and $Z_r = \sqrt{L_r/C_r}$ as the base values:

$$i_{L_r-pu}(t) = i_{L_r}(t) \frac{Z_r}{V_{in}} = \left(C e^{-\alpha t} \cos(\omega_r t - \phi_1) + D_1 t + D_0 \right) \frac{Z_r}{V_{in}}$$

$$= C^* e^{-\alpha t} \cos(\omega_r t - \phi_1) + D_1^* t + D_0^* \quad (13)$$

where

$$D_1^* = D_1 \frac{Z_r}{V_{in}}, \quad D_0^* = D_0 \frac{Z_r}{V_{in}}, \quad B^* = B \frac{Z_r}{V_{in}};$$

$$A^* = A \frac{Z_r}{V_{in}}, \quad C^* = C \frac{Z_r}{V_{in}}, \quad \phi_1^* = \phi_1 \frac{Z_r}{V_{in}}.$$

The normalized capacitor voltage is obtained by considering V_{in} as the base value:

$$v_{C_{r-pu}}(t) = v_{C_{r-pu}}(t) \frac{1}{V_{in}} = \frac{L_r}{V_{in}} (E e^{-\alpha t} \cos(\omega_r t - \phi_2) + D_1) \frac{Z_r}{Z_r}$$

$$= K \left(E^* e^{-\alpha t} \cos(\omega_r t - \phi_2^*) + \frac{K^2 - 1}{K^3} \right) \quad (14)$$

where

$$E^* = -\sqrt{\left(\frac{C^*}{2Q}\right)^2 + (C^*)^2}; \quad \phi_2^* = \phi_1^* - \text{tg}^{-1}(2Q).$$

Normalized input current:

$$i_{Lin-pu}(t) = i_{Lin}(t) \frac{Z_r}{V_{in}} \quad (15)$$

$$= \omega_n (K^2 - 1) \cdot t - (K^2 - 1) (i_{L_{r-pu}} - I_{L_{r-pu}}(0)) + I_{in-pu}(0).$$

Once the relations for one-half switching cycle were established, the cycle-by-cycle operation of the CFPPRI was analyzed. This was accomplished by considering the initial conditions of the next cycle as the last state of the previous one and repeating the calculations for the next cycle with the proper notation as was described above. Fig. 4 shows the normalized cycle-by-cycle waveforms of the CFPPRI for the case of switched load (numerical calculations were carried out by MATLAB 6).

Using the normalized relations, some important characteristics of the CFPPRI can be brought out: Fig. 5 shows the output voltage sag due to a step perturbation of the load as a function of the quality factor for several inductor ratios. Fig. 6 shows the delay time till the overshoot maxima that occurs after a load step was applied.

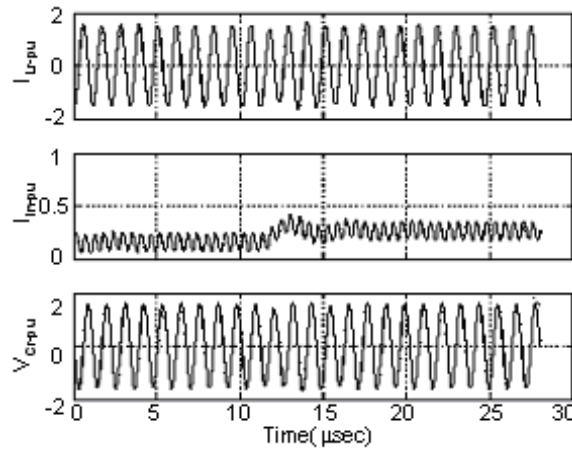


Figure 4: Cycle-by-cycle step response waveforms for the load switched from 100% to 60%.

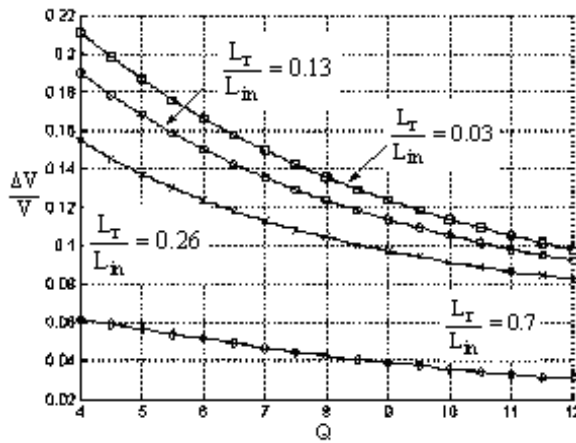


Figure 5: Output voltage sag for a 100% to 60% step of the load as a function of Q for several ratios of K (L_r/L_{in}).

All the relations above were derived under the assumption that the switching frequency and the resonant frequency are equal. However, in many practical applications, an exact matching is not possible. Interconnecting cable capacitances, tolerances of the passive components, and variability of the

load reactance will cause the CFPPRI to operate in one of the mismatched modes that were described above.

The sensitivity of the CFPPRI to frequency deviation can be eliminated by incorporating a frequency tracking mechanism, along with a variable inductor and introduce a Self-Adjusting CFPPRI [1, 2] that will also provide the ability of driving the load with a predetermined frequency, controlled by the user.

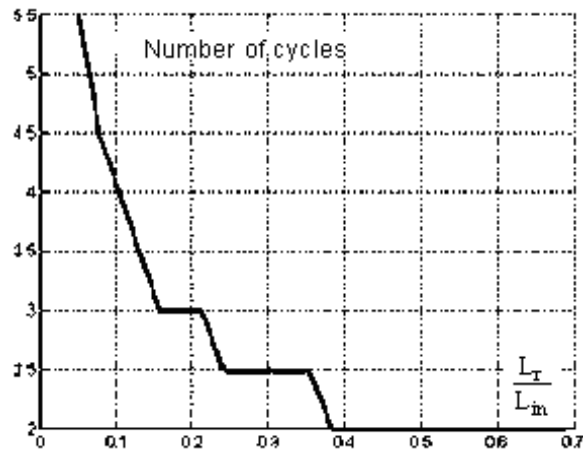


Figure 6: Number of switching cycles that passes from a step perturbation of the load to overshoot of the output voltage as a function of K (L_r/L_{in}).

3 The self-adjusting current-fed push-pull parallel resonant inverter (SA-CFPPRI)

Since the details of the SA-CFPPRI were given earlier [2,3], we present here only a brief description of this power source.

The SA-CFPPRI is built around a self-oscillating inverter (Fig. 7) that comprises two switches (Q1, Q2) and a Soft Switching Control (SSC) assembly. The SSC keeps the inverter at the resonant frequency by switching the drive whenever the center tap voltage (V_{tap}) reaches zero. This control method is based on the concept used in the IC design of Texas Instrument's (originally Unitrode) controller UC3872 [5,6]. When locked, the SSC ensures zero voltage switching of the SA-CFPPRI while the frequency of operation is determined by the equivalent capacitance and inductance of the resonant tank (L_r, C_2, C_3 and C_L). Changing the inductance of L_r can thus change

the operating frequency. This is accomplished in the SA-CFPPRI by incorporating a high frequency variable inductor T1 (Fig. 7). The inductor [2,3,7] is based on an E core with gaped center leg and bias windings on the non-gaped side legs. The variable inductor is controlled by a bias current that is fed to the bias winding using a Buck type converter (Fig. 7) that operates in closed loop around amplifier A1 to maintain a controlled signal. Frequency tracking of the SA-CFPPRI is then assured by incorporating a phase comparator that generates an error signal as a function of the phase difference between the desired frequency F_{in} and the running frequency of the PPRI, F_{β} . A phase deviation will change the bias current of the variable inductor and hence cause F_{β} to follow F_{in} .

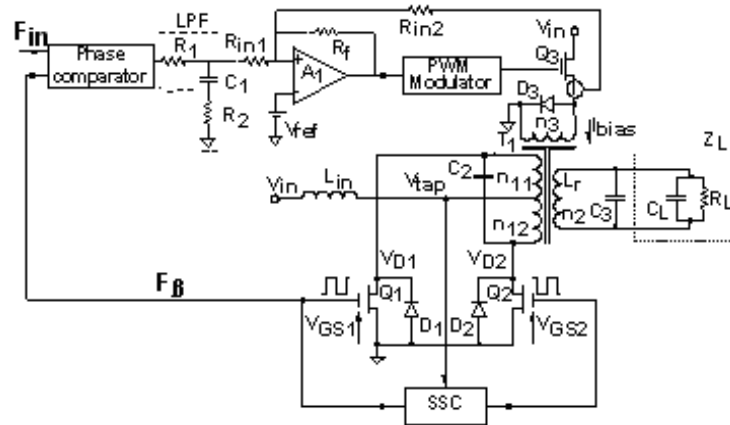


Figure 7: The SA-CFPPRI system.

The bias drive of the SA-CFPPRI is designed as closed feedback loop configuration to maintain a forced current control. This is required to reduce the order of the outer feedback loop. A detailed dynamic analysis of the inverter for the system response and stability criteria of the feedback loops is given in [2].

4 The SA-CFPPRI performance under switched load conditions

A prototype SA-CFPPRI was previously simulated and tested experimentally for the ability to maintain a constant output signal under load changes.

In this study, we tested the performance of the SA-CFPRI when connected to a switched load. The load circuit setup consists of two resistors connected in series while one of the resistors is paralleled with an IRF840 power MOSFET. The resistance values were chosen to cause a step in the output power from a full power of 5W (when the switch is turned on) to 60% of the full output power – 3W (when the switch is turned off). The target parameters of the experimental unit were: input voltage 11VDC; output voltage $V_{out} = 160$ Vrms; load capacitance $C_L = 2.1$ nF; output frequency 93 kHz.

Fig. 8 shows the experimental response of the SA-CFPRI to a 60% to 100% step in the output power. The output signal is stabilized after three HF cycles, a voltage dropout of 10% was measured at the first half cycle after the step was applied. No steady state error was observed.

The efficiency of the experimental unit (taking into account the total input power to power stage and control section) was found to be about 67% when the inductors bias current was low and about 52% when the variable inductor was forced to its minimum value (highest bias current).

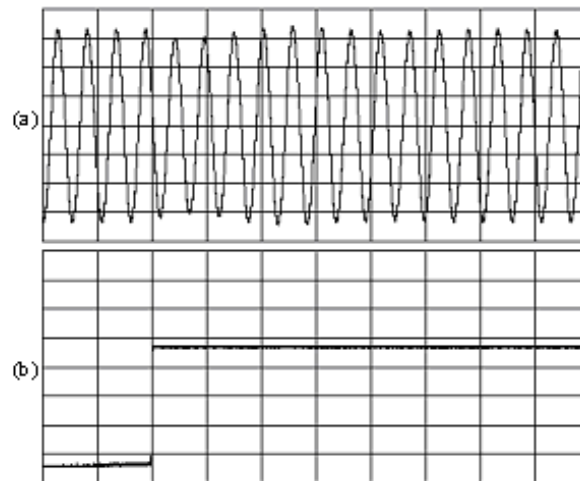


Figure 8: Response of experimental unit to a step from 60% to 100% of the output power. (a) output voltage, 70V/div and (b) V_{GS} of Q_L of Fig. 2, 5V/div; horizontal scale: 20μ s/div.

5 Discussion and conclusions

The SA-CFPPRI was shown to be able to keep a stable sinusoidal output signal even when the load power changes, and thus satisfies the demand of a power source for AC distributed power system bus. Another benefit of the proposed power source is the ability to maintain a constant output frequency being connected to reactive loads. Possible uses for this type of inverters include medical instrumentation and other applications where multiple floating power supplies are needed.

The normalized analysis presented here, provide the designers a useful tool in designing and optimizing features of the HFAC bus driver and CFPPRI topologies when feeding switched loads.

The voltage sag was shown to be dependent on the quality factor (Q) inversely, that is, high Q will minimize the voltage sag. However, one should be aware that in a high Q system the reactive current that circulates in the resonant tank would cause extra power losses. This deficiency limits the range of the output power level of the proposed power source to low or medium power (hundreds of Watts) and may not be practical in high power applications due to the high circulating current of the tank.

The proposed topology is classified as underdamped system, since it is of high Q ($Q > 5$). This implies that for a step perturbation of the load the CFPPRI will oscillate. However, the results of the present study show that the oscillations will be negligibly small compared to the signal, after the first overshoot occurs. That is, the settling time is practically equal to the delay until the first overshoot occurs.

Considering the above, the SA-CFPPRI as a HFAC bus driver provides the ability of hot-plug-in, that is, loads may be taken in and out, while the driver the driver maintains a constant, sinusoidal supply signal.

This research was supported by The Israeli Science Foundation (grant No. 113/02) and by the Paul Ivanier Center for Robotics and Production management.

References

- [1] R. Watson, W. Chen, G. Hua, and F.C. Lee, VPEC Power Electronics Seminar Proceedings, p.11 (1995).
- [2] S. Ben-Yaakov and M.M. Peretz, IEEE Applied Power Electronics Conference, APEC'04, Anaheim, p.1832 (2004).

- [3] S. Ben-Yaakov and M.M. Peretz, Power Electronics Specialists Conference, PESC'04, Aachen, p.61 (2004).
- [4] G. Ivensky, A. Abramovitz, M. Gulko, and S. Ben-Yaakov, IEEE Trans. on Aerospace and Electronic Systems **29**, 926 (1993).
- [5] *Resonant lamp ballast controller*, UC3872 data sheet, Unitrode, Texas Instruments. <http://focus.ti.com/lit/ds/symlink/uc3872.pdf>
- [6] E. Wells, *Using the UC3871 and UC3872 Resonant Fluorescent Lamp Drivers in Floating Lamp Applications*, UC3872 application notes, Unitrode, Texas Instruments. <http://focus.ti.com/lit/an/slua090/slua090.pdf>
- [7] D. Medini and S. Ben-Yaakov, IEEE Applied Power Electronics Conference, APEC'94, Orlando, p.219 (1994).